International Journal of Advanced Research in Physical Science (IJARPS)
Volume 8, Issue 3, 2021, PP 1-15
ISSN No. (Online) 2349-7882
www.arcjournals.org

Thomson-Benard phenomena and Relaxed Optics

Petro P. Trokhimchuck *

Anatoliy Svidzinskiy Department of Theoretical and Computer Physics, Lesya Ukrayinka Volyn' National University, 13 Voly Avenue, 43025, Lutsk, Ukraine

Corresponding Author:** ***Petro P. Trokhimchuck, *Anatoliy Svidzinskiy Department of Theoretical and Computer Physics, Lesya Ukrayinka Volyn' National University, 13 Voly Avenue, 43025, Lutsk, Ukraine*

Abstract: *Main peculiarities of Bernard phenomena are discussed. Corresponding models and theories, which are used for the explanation this phenomenon, are represented. Questions about possible observation these phenomena in Relaxed optics are analyzed.*

Conditions for the regimes of laser irradiation and irradiated matter, which are necessary for the creation and observation the Bernard phenomena are formulated and discussed. Role and possible applications these phenomena in laser technology and modern optoelectronics are analyzed too.

Keywords: *Thomson-Bernard phenomena, laser irradiation, filaments, Rayleygh, liquids, Chandrasekar, hexagonal structures, laser technology, ssemiconductors.*

1. INTRODUCTION

First observation the phenomena of creation polygonal forms in heated liquid was made by count Rumford in 1797 [1-3]. In 1870, the Irish-Scottish physicist and engineer James Thomson, observed water cooling in a tub; he noted that the soapy film on the water's surface was divided as if the surface had been tiled (tesselated). In 1882, he showed that the tesselation was due to the presence of convection cells [4]. In 1900, the French physicist Henri Bénard independently arrived at the same conclusion [5, 6]. This pattern of convection, whose effects are due solely to a temperature gradient, was first successfully analyzed in 1916 by Lord Rayleigh [1, 3, 6-8]. Rayleigh assumed boundary conditions in which the vertical velocity component and temperature disturbance vanish at the top and bottom boundaries (perfect thermal conduction). Those assumptions resulted in the analysis losing any connection with Henri Bénard's experiment. This resulted in discrepancies between theoretical and experimental results until 1958, when J. Pearson reworked the problem based on surface tension [9]. This is what was originally observed by Bénard. Nonetheless in modern usage "Rayleigh–Bénard convection" refers to the effects due to temperature, whereas "Bénard–Marangoni convection" refers specifically to the effects of surface tension. Davis and Koschmieder have suggested that the convection should be rightfully called the "Pearson–Bénard convection". Rayleigh–Bénard convection is also sometimes known as "Bénard–Rayleigh convection", "Bénard convection", or "Rayleigh convection" [10-16].

The experimental set-up uses a layer of liquid, e.g. water, between two parallel planes. The height of the layer is small compared to the horizontal dimension. At first, the temperature of the bottom plane is the same as the top plane [1, 6]. The liquid will then tend towards an equilibrium, where its temperature is the same as its surroundings. (Once there, the liquid is perfectly uniform: to an observer it would appear the same from any position. This equilibrium is also asymptotically stable: after a local, temporary perturbation of the outside temperature, it will go back to its uniform state, in line with the second law of thermodynamics).

Then, the temperature of the bottom plane is increased slightly yielding a flow of thermal energy conducted through the liquid. The system will begin to have a structure of thermal conductivity: the temperature, and the density and pressure with it, will vary linearly between the bottom and top plane. A uniform linear gradient of temperature will be established.

Once conduction is established, the microscopic random movement spontaneously becomes ordered on a macroscopic level, forming Benard convection cells, with a characteristic correlation length.

The experimental set-up uses a layer of liquid, e.g. water, between two parallel planes. The height of the layer is small compared to the horizontal dimension. At first, the temperature of the bottom plane is the same as the top plane. The liquid will then tend towards an equilibrium, where its temperature is the same as its surroundings. (Once there, the liquid is perfectly uniform: to an observer it would appear the same from any position. This equilibrium is also asymptotically stable: after a local, temporary perturbation of the outside temperature, it will go back to its uniform state, in line with the second law of thermodynamics).

The rotation of the cells is stable and will alternate from clock-wise to counter-clockwise horizontally; this is an example of spontaneous symmetry breaking. Bénard cells are metastable. This means that a small perturbation will not be able to change the rotation of the cells, but a larger one could affect the rotation; they exhibit a form of hysteresis.

Moreover, the deterministic law at the microscopic level produces a non-deterministic arrangement of the cells: if the experiment is repeated, a particular position in the experiment will be in a clockwise cell in some cases, and a counter-clockwise cell in others. Microscopic perturbations of the initial conditions are enough to produce a non-deterministic macroscopic effect. That is, in principle, there is no way to calculate the macroscopic effect of a microscopic perturbation. This inability to predict long-range conditions and sensitivity to initial-conditions are characteristics of chaotic or complex systems (i.e., the butterfly effect) [1, 3, 6, 9-17].

If the temperature of the bottom plane was to be further increased, the structure would become more complex in space and time; the turbulent flow would become chaotic.

Convective Bénard cells tend to approximate regular right hexagonal prisms, particularly in the absence of turbulence, although certain experimental conditions can result in the formation of regular right square prisms or spirals.

The convective Bénard cells are not unique and will usually appear only in the surface tension driven convection. In general the solutions to the Rayleigh and Pearson analysis (linear theory) assuming an infinite horizontal layer gives rise to degeneracy meaning that many patterns may be obtained by the system. Assuming uniform temperature at the top and bottom plates, when a realistic system is used (a layer with horizontal boundaries) the shape of the boundaries will mandate the pattern. More often than not the convection will appear as rolls or a superposition of them.

Since there is a density gradient between the top and the bottom plate, gravity acts trying to pull the cooler, denser liquid from the top to the bottom. This gravitational force is opposed by the viscous damping force in the fluid. The balance of these two forces is expressed by a non-dimensional parameter called the Rayleigh number. The Rayleigh number is defined as [1-3]:

$$Ra = \frac{g\alpha\beta}{\kappa\nu} d^4, \tag{1}$$

where g denotes the acceleration due to gravity, d the depth of the layer, $\beta = \left| {}^{dT}\!/_{dz} \right|$ the uniform adverse temperature gradient which is maintained, and α, κ and ν are the coefficients of volume expansion, thermometric conduictivity and kinematic viscosity, respectively [1, 2].

As the Rayleigh number increases, the gravitational forces become more dominant. At a critical Rayleigh number of 1708, instability sets in and convection cells appear.

The critical Rayleigh number can be obtained analytically for a number of different boundary conditions by doing a perturbation analysis on the linearized equations in the stable state. The simplest case is that of two free boundaries, which Lord Rayleigh solved in 1916, obtaining Ra = ${}^{27}\!/_{4}\,\pi^4 \approx 657.51$. In the case of a rigid boundary at the bottom and a free boundary at the top (as in the case of a kettle without a lid), the critical Rayleigh number comes out as Ra = 1100.65 [1, 6].

Further development of problem of hydrodynamic stability was made by S. Chandrasekar in magnetic hydrodynamics. These results allow explaining the basic peculiarities of generation the Sun spots and its dynamics [1].

Model of polygonal forms Thomson-Benard cells was created by H. Haken [12].

The theory of Thomson-Benard phenomena for electron gas in semiconductors was created and developed by V. Bonch-Bruevich and A. Temchin [18-21].

Roughly speaking the Thomson-Benard phenomena is hydrodynamical effect, which is generarated on the early stage of formation the hydrodynamical vortexes. It is"soft" effect. Therefore for the observation this phenomenon we must select slow regime of laser-induced melting the irradiated matter. This should be a relatively long-term process, which would include the melt of the irradiated material, its heating, and the initiation of convective fluid motion. We believe that the most suitable laser irradiation regimes can be continuous, millisecond and microsecond irradiation regimes [3, 22-28]. Silicon, germanium and titanium were selected as possible materials. A comparative analysis with the cascade physical-chemical model of laser-induced transformation [22-28] is carried out. A significant difference in obtaining the laser-induced Thomson-Benard phenomenon and physicochemical phase transformations is shown.

2. EXPERIMENTAL DATA

The earlier experiments to demonstrate in a definitive manner the onset of thermal instability in fluids are those of Benard in 1900, though the phenomenon of thermal convection itself had been recognized earlier by count Rumford (1797) and James Thomson [4] (Fig. 1).

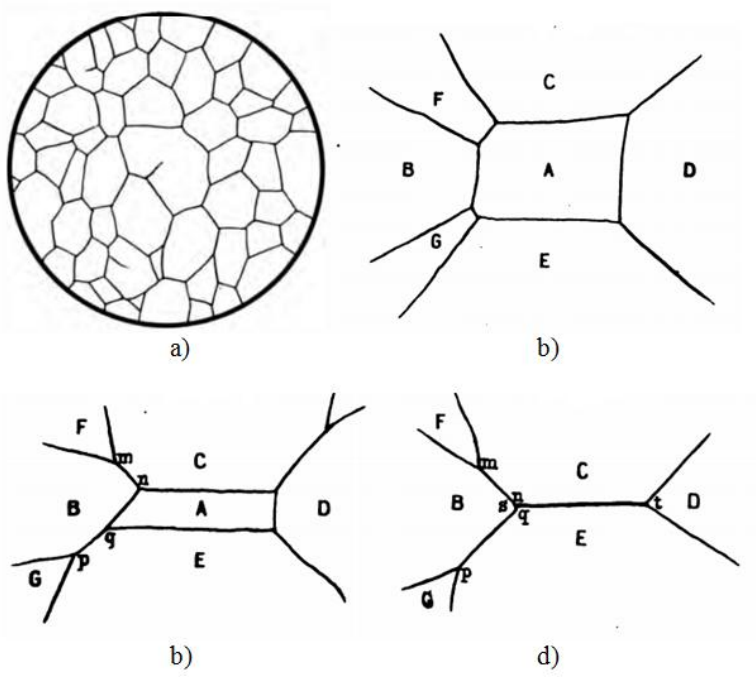

Fig1. *Thomson cells [4].*

Fig 1a represents the general appearance that the surfacer of the soapy water in the pan would usally exhibit when left standing in the manner described. By continuous watching, it may be noticed that the smaller enclosed patches are general diminishing in size, being encroached on by the larger ones until the collapse and cease to exist. At the same time the lerge ones show tendencies to sever themselves into to or more new ones, which in thir turn either increase and split again, or diminish and go out of existence. To describe the numerous and varied features of transition in words would not be easy, but Fig. 1b, 1c and 1d show three successive conditions which have been observed as occurring.

In Fig 1b the patch A has larger neighbours – B, C, D, and E – contiguous with it, and it has also two narrow patches – F and G – contiguous with small portion of its boundary. The patch A is comparatively narrow in the direction between C and E, and is rapidly encroached on by those two large patches C and E, and becomes narrower than before, without necessarily being shortened in length.. Also, during the same time, the narrow patches F and G collapse, each in nits place of meeting with the boundary of A; and in each case where the collapse takes place a bounding line is left between the two, which come together, as is shown by *m n* and *p q* in Fig. 1c, the patches F and G

of Fig. 1b having retired to their new positions, shown as F and G in Fig. 1c. A little later, and the patch A is observed to have disappeared entirely, by collapsing into the line s t in Fig. 1d [4].

Multitudinous varieties of changes, partaking more or less of the general character of those here described, may be noticed in various watchings of the behaviour of the soapy liquid from time to time. The patches, with their boundaries, when viewed with favourably applied light, show appearances as if each patch were formed as the top of column of slowly rising fluid, having a morther-of-pearl-like luster, and with a thin layer of more translucent liquid lying on the tops of these pearly patches. It seems to be that there is on the whole a very slow ascending motion in these columnar spaces, and that above, there is a thin superficial layer of cooler and seemingly more translucent liquid, receiving perpetually new supplies from the rising substance of those columns, and flowing outwards over each column top, and that the two sheets, spreading out on each of two contiguous columns, plunge downwards, where they meet in the mutual bounding line of the two spaces or column tops, the downward current seems to be more active that at the over parts of the septums. The various ascending flows here spoken of as columns, or columnar spaces, for want of any better nomenclature, may probably not exist like separate columns with septums between them of descending liquid except near the surface. It seems likely that the down-flowing of the so-colled septums may tend to gather into thicker streams descending from the corners of the surface patches where three of such spaces meet; but the internal motions, being concealed from view, remain as yet obscure, and in a great degree unknown.

Further experiments were received by Benard and other researches. It will suffice to summarize here the principal facts established by them. They are: first, a certain critical adverse temperature gradient must be exceeded before instability can set in; and second, the motions which ensue on surpassing the critical temperature gradient have a stationary cellular character. What actually happens at the onset of instability is that the layer of fluid resolves itself into the number of cells; and if the experiment is performed with sufficient care, the cells become equal and they align themselves to form a regular hexagonal pattern.

H. Benard used the expression tourbillons cellulaires, which are later known as Benard cells [5, 6]. He insisted on polygonal characteristics of this cellular, semi-regular vortex due to existence of polygons of four, five, six, and seven sides, but with a predominance of hexagons [6]. He pointed out the difficulty of producing regular hexagons on a long surface withiot many defects. These cellular vortices could be generated in a steady state, under a moderate heat flux. Benard also observed vortices in fairly valotile liquids, sush as alcohol or hydrocarbon, underlying the fact, that the evaporation chilled the surface, causing the vertical heat flux. [6]. In order to produce a uniforrn thickness and to avoid evaporation problems, he worked with higher temperatures, between 50° C and 100° C, using substances which melted at 50° C such as wax or spermaceti, a whale oil, which melts at 46° C, but has no significant valotility below 100° C. This allowed him to create liquid films of one millimeter thickness controlled bto with one micron and to obtain a spread of the thin layers , which remain constants for many hours [6].

H. Benard had possibility to measure thickness differences of 1 micrometer for liquid layers and of 1 milimeter for spermaceti at an average temperature 100° C.

Fig. 2 (which is a reproduction of one of Benard's early photogaths) illustrates this phenomenon.

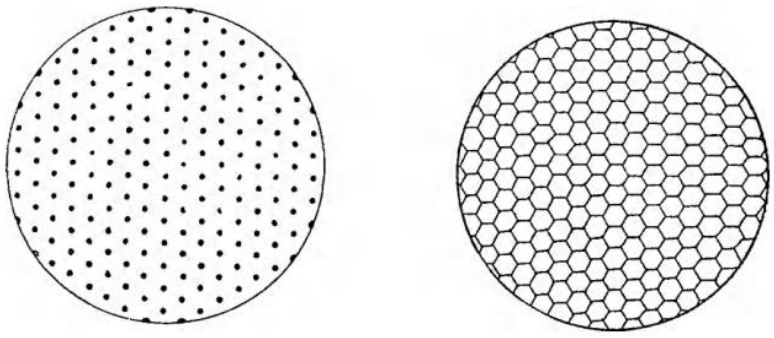

Fig2. *Benard cells in spermaceti. Cells visualization by reflection and transmission: temperature 61.36° C, thickness – 0.64 mm [5, 6].*

The typical Benard convection cells are represented in Fig. 3 [6].

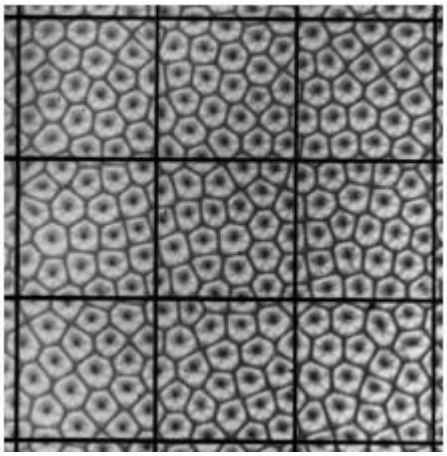

Fig3. *Convection cells [6]*.

The layer rapidly resolves itself into a number of cells, the motion being an ascession in the middle of cell and a descension at the common boundary between a cell and its neighbors. Two phases are distinguished, of unequal duration, the first being relatively very short. The limit of thr first phase is described as the "semi-regular regime"; in this state all the cells have already acquired surfaces nearly identical, their forms being nearly regular convex polygons of, in general, 4 to 7 sides. The boundaries are vertical, and the circulation in each cell approximate to that already indicated. This phase is brief (1 or 2 seconds) for the less viscous liquids (alcohol;, benzene, etc.) at ordinary temperatures. Even for paraffin and spermaceti, melted at 100°C, 10 seconds suffice; but in the case of very viscous liquids (oils, etc.), if the flux oh heat is small, the deformations are extremely slow and the firs phase may last several minutes or more.

The second phase has for its limit a permanent regime of regular hexagons. During this period the cells become equal and regular and align themselves. It is extremely protracted, if the limit is regarded as the complete attainment of regular hexagons. And, indeed, such perfection is barely attainable even with the most careful arrangements. The tendency, however, seems sufficiently established.

According by H. Haken [12] Thomson-Bernar phenomena are one with set processes of hydrodynamic instability. So, results of Fig. 2 are corresponded to small Ruyleygh numbers. The picture of hydrodynamic instability for great Rayleygh numbers is represented in Fig. 4.

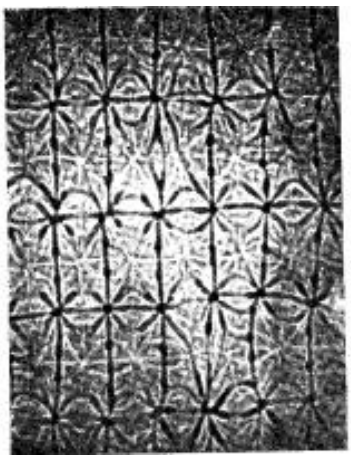

Fig4. *Structures for great Rayleyghs numbers [12]*

3. MODELING AND DISCUSSIONS

The theoretical foundations for a correct interpretation of the foregoing facts were laid by Lord Rayleygh in a fundamental paper [7]. Rayleygh showed that what decides the stability, or otherwise, of a layer fluid heated from below is the numerical value of the non-dimensional parameter (1), Rayleygh number *Ra*.

Rayleygh further showed that instability must set in when *Ra* exceeds a certain critical value Ra_c; and that when *Ra* just exceeds Ra_c, a stationary pattern of motions must come to prevail. The principal theoretical question is therefore: how is one to determine Ra_c?

For resolution of this problem system of equations of hydrodynamics and thermo conductivity with corresponding boundary conditions were used.

We explain basic peculiarities of Thomson-Benard phenomena with using Bussinesq approximation [1-3].

According [1-3] basic system of equations in this approximation may be represented in next form:

$$\frac{\partial \rho}{\partial t} + u_j \frac{\partial \rho}{\partial x_j} = -\rho \frac{\partial u_j}{\partial x_j}, \tag{2}$$

$$\frac{\partial T}{\partial t} + u_j \frac{\partial T}{\partial x_j} = \kappa \Delta T - \frac{p}{\rho c_V} \frac{\partial u_j}{\partial x_j} + \frac{1}{\rho c_V} \Phi, \tag{3}$$

$$\rho \frac{\partial u_i}{\partial t} + \rho u_j \frac{\partial u_i}{\partial x_j} = -\frac{\partial p}{\partial x_i} + \frac{\partial}{\partial x_j} \left\{ \mu \left(\frac{\partial u_i}{\partial x_j} + \frac{\partial u_j}{\partial x_i} \right) - \frac{2}{3} \mu \frac{\partial u_j}{\partial x_j} \right\} - g \rho \lambda_i. \tag{4}$$

Where p – pressure, T – temperature, u – velocity of fluid in prturbated state, c_V – specific heat capacity for stable volume, μ – dynamical viscosity, Φ – viscous dissipation, λ_i – the unit vector of proper direction.

Let the altered temperature distribution be

$$T' = T_0 - \beta \lambda_j x_j + \theta. \tag{5}$$

In the unperturbated state

$$\frac{\partial \rho}{\partial x_j} = \lambda_j \rho_0 \alpha \beta; \tag{6}$$

and the change in the density δp caused by the perturbation Θ in the temperature is given by

$$\delta p = -\alpha \rho \theta = -\alpha \rho_0 \left(1 + \alpha \beta \lambda_j x_j\right) \theta. \tag{7}$$

The analysis of these system equations in approximation of normal modes gives next equations [2, 3]:

$$\left(D^2 - a^2\right)\left(D^2 - a^2 - \sigma\right) W = \left(\frac{g\alpha}{\nu} d^2\right) a^2 \Theta, \tag{8}$$

$$\left(D^2 - a^2 - \Pr \sigma\right) W = -\left(\frac{\beta}{k} d^2\right) W, \tag{9}$$

where $D = \frac{d}{dz}$ and $\Pr = \frac{\nu}{k}$ is the Prandtl number.

The associated boundary conditions are

$$\Theta = 0, W = 0 \text{ for } z = 0 \text{ and } 1, \tag{10}$$

and

$$DW = 0 \text{ for } z = 0 \text{ and } 1 \tag{11}$$

if both bounding surfaces are rigid or

$$DW = 0 \text{ for } z = 0 \text{ and } D^2W = 0 \text{ for } z = 1 \tag{12}$$

if the bottom surface is rigid and the top surface is free.

By eliminating Θ between the equations (8) and (9), we obtain

$$\left(D^2 - a^2\right)\left(D^2 - a^2 - \sigma\right)\left(D^2 - a^2 - \Pr \sigma\right) W = Raa^2 W, \tag{13}$$

where Ra is Rayleigh number (1).

An identical equation governs Θ.

The instability of Rayleygh numbers for first even and first odd modes is represented in Fig. 4.

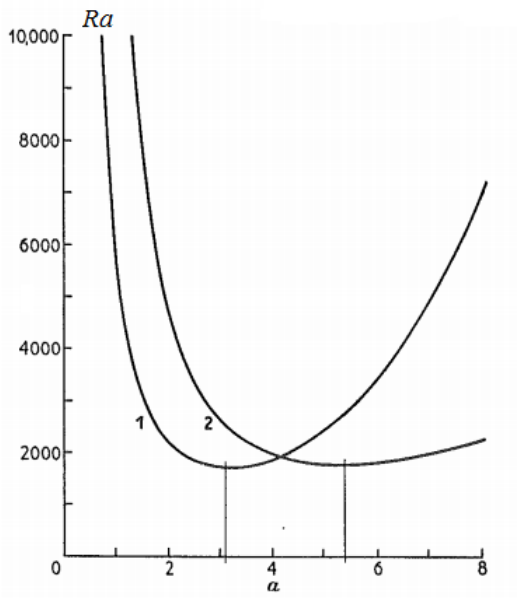

Fig4. *The Rayleygh number at which instablility sets in for disturbances of different wave numbers a for the first even (curve labeled 1) and the first odd (curve labeled 2) mode [2, 3].*

The proper solutions for W (curve 1) and $(a^2Ra)^{-2/3}F$ (curve 2) for the state of marginal stability for the case when both bounding surfaces are rigid [2, 3] are represented in Fig. 5. Where F is $F(\infty\Theta)$ [2].

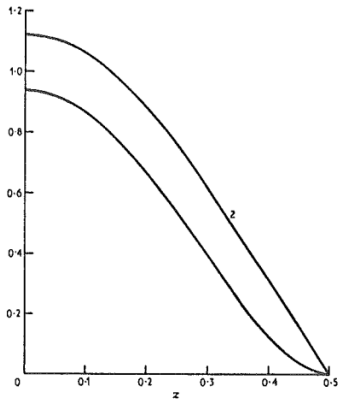

Fig5. *The proper solutions for W (curve 1) and $(a^2Ra)^{-2/3}F$ (curve 2) for the state of marginal [2].*

The described phenomenon was investigated by Bénard " as long ago as the beginning of the present century. In recent times It has attracted attention for a number of reasons—among them the extremely fundamental characteristic: this is an example of the formation of an ordered structure as the result of an external influence, essentially deriving the system from a state of thermodynamic equilibrium."

It is interesting to investigate whether it is possible to realize a somewhat similar situation in regard to the gas of charge carriers in a semiconductor [18-21]. Of course, here an electric field might play the role of the gravitational field. The reasons for posing this problem are clear: a periodic distribution of the electron temperature and (or) of the concentration of charge carriers (with a period exceeding the mean free path with respect to momentum) would imply that various macroscopic characteristics of the system are also periodically dis- tributed, among them the electrical conductivity, the light absorption coefficient, etc. with obvious consequences [18].

Heating of an electron gas can be achieved even with- out the participation of a static field-with the aid of light (this possibility has been investigated in a different context by a number of author [21]).

Thus, we arrive at the scheme represented in the Fig 6 [18]. There the force acting from the side of the externally applied electric field 1s denoted by F. It is necessary, however, to keep in mind that the carriers redistribution due to compression of the electron gae may lead to the appearance of an additional field in the sample. The latter, of course, impedes the effect of interest to us,

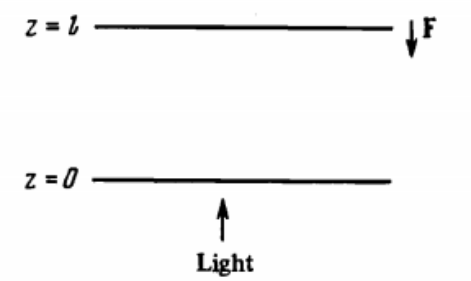

Fig6. *The sample is bounded by the planes z = 0 and z = l and is infinite in the x and y directions. The half-spaces z <0 and z > l are occupied by dielectric media [18].*

In the present article we shall consider a monopolar semiconductor under conditions in which the characteristic times of interelectron collisions (τ_{ee})› mmmentum relaxation (τ_p)t and energy relaxation (τ) satisfy the inequalities

$$\tau_p << \tau_{ee} << \tau. \qquad (14)$$

In this connection the concept of an electron temperature T has a unique meaning, and all kinetic coefficients depend on *T*. The latter fact allows us to avoid the complications indicated above, which are related to the compression of a gas of charged particles. In fact, a new mechanis for variation of the pressure appears in the conditions under consideration, resulting from the temperature dependence of the energy relaxation time and the temperature dependence of the thermal conductivity κ of the electron gas: it is obvious that the pressure of the electron gas is very Strongly increased in the lower part of the sample" (see the figure) for $d\tau/dT > 0$ and $d\kappa/dT > 0$. In this connection the compressibllity of the gas can generally be neglected, whlch we therefore do. Consequently the presence of an external field is no longer compulsory (although it may turn out to be of some use); here we assume F = 0.

The absorption of warming light in the conditions under consideration must be caused by intraband transitions. In this connection energy is put into the electron gas, but new charge carriers do not appear, and the redistribution of the electrons in space aleo does not play an important role.

Under conditions (14) the fundamental equations of the problem are the equation of continuity, the expression for the current density j, the energy transport equation, and equation Poisson's equation. Let us introduce the following notation: n denotes the carrier concentration; δn denotes its small fluctuation; $u = j/en$ is the drift velocity; T_0 is the lattice temperature (expressed in energy units, just like *T*); α is the differential thermo e.m,f.; μ is the mobility ($\mu \sim T^r$, where *r* is a known number); *m* is the effective mass; ε is the dielectric constant of the sample; γ is the coefficient for the absorption of the "warming" light; J(z) denotes the flux of light energy into the sample, and J_m 1s Its value at z = +0.

It is clear that three characteristic lengths exist in the problem: *l*, γ^{-1}, and $\lambda_0^{-1} = \left(2\kappa_0\tau_0/3\right)^{1/2}$ (the subscript 0 denotes the corresponding quantity in the absence of heating (for $T = T_0$)). Depending on the relationships between them, the following cases are dtstinguiahed:

a) surface absorption, a "thin'' sample: $\gamma^{-1} << l << \lambda_0^{-1}$; b) surface absorption, a "thick" sample: $\gamma^{-1} << \lambda_0^{-1} << l$; c) bulk absorption: $\gamma^{-1} >> \lambda_0^{-1}$.

In cases a) and b) the absorption of light energy can be taken into consideration with the aid of the boundary condition ‹xi the equation of energy transport; in case c) the absorption must be taken into consideration in this equation itself. The latter sltuation is evldently encountered most frequently, and it is the only case which wiH be explicitly treated in [18]. One can show, however, that results analogous to those indicated below are obtained for surface absorption. We shall also assume that $l >> \gamma^{-1}$. In this connection the sample can be regarded as "infinitely thick."

Thus, in the case of a nondegenerate gas the equations for the problem have the form

$$div\vec{u} = 0, \tag{15}$$

$$\vec{u} = \mu\vec{E} - \mu\alpha\nabla T, \tag{16}$$

$$\partial T/\partial t + \frac{1}{3}(5+2r)div(\vec{u}T) - \frac{2}{3}e\vec{u}\vec{E} - \frac{2}{3}div(\kappa\nabla T) + (T-T_0)/\tau = \frac{2}{3}n^{-1}\gamma J(z), \tag{17}$$

$$div\vec{E} = 4\pi e\delta n/\varepsilon. \tag{18}$$

Formula (16) is obtained from the well known expression for the current density [18, 21]:

$$\vec{j} = en\mu(T)\left\{\vec{E} - \frac{T}{en}\nabla n - \alpha(T)\nabla T\right\}. \tag{19}$$

Here the gradient In is taken at constant temperature. The approximation of incompressibllity assumed by us consiate, as uaual, of neglecting the second term inside the curly brackets (retaining the possibility of changes in n due to a variation of the temperature *T*). Poisson's equauon (18) is the only equation where it is necessary to take the small change of the electron concentration into consideration. As is customary in such a formulation of the problem, in what follows it will be utilized in order to estimate 6n and to establish the eondltiona for applicability of the quaaineutrality approximation,

The boundary conditions on Eqs. (15) − (18) are the usual eontinulty condidons for *E* (they determine the field outside the sample), the conditions of boundedness of all quantities upon unlimited (in absolute value) growth of the coordinates x, y, and z, and the equations

$$u_z = 0, \quad z = 0, \tag{20}$$

$$-n\kappa\,\partial T/\partial z = \nu n(T - T_0), \quad z = 0. \tag{21}$$

Here ν ia a phenomenologically introduced positive coefficient (having the dimensions of a velocity), which characterizes the heat exchange between the electron gas in semiconductor and in the dielectyric medium adjacent to it. For too not large difference between *T* and T_0, in order of magnitude one has

$$\nu \approx \left(\frac{T}{m}\right)^{1/2} P, \tag{22}$$

Where *P* is the probability for the passage of an electron through of contact.

According to [18] critical value of the energy flux, the value at which the considered change in the state of electron gas takes place

$$J_c = 3nT_0/2\gamma\tau_o(2\dot{\tau} + \dot{\kappa}). \tag{23}$$

We note, that $\gamma/n = \sigma$, where σ is the cross section for photon absorption.

For n- InSb [18] this formula give value for $T = 3K$

$$J_c = \frac{2,5}{2\dot{\tau} + \dot{\kappa}} \cdot 10^{-2}\left[\frac{W}{cm^2}\right]. \tag{24}$$

In this material $\sigma \approx 2.3 \cdot 10^{-17} \left(\lambda / 2\mu \right)^2$ for a wave length $\lambda \geq 9\mu$. For $\lambda = 300\mu$ this gives $\sigma \approx 2.5 \cdot 10^{-14} cm^{-2}$.

The hexagonal forms of Thomson-Benard cells are characterized only thin layers. This question was resolved by Rayleygh [7] and H. Haken [12]. Haken investigated the problem of stability of different modes. According to [12] one-mode confiquration have maximal stability. Haken received that of stable configuration have cylindrical and hexagonal forms. Rayleygh accented attention on hexagonal forms as maximal stable phases too [7]. From microscopic point of view this hexagonality is display of the molecular structure of a substance [3, 26]. Triangle water molecules are created the hexagonal monolayers; organic media included hexagonal elements of its structure. Threfore for heatind thin layers with few monolayers begin oscillate and on the begin stage of generation the vortexes its borders have hexagonal forms (symmetry of molecules influence on the symmetry of cells) [3, 26]. These thin layers have some analogy with graphen and silicen [29]

4. Possible Observations And Applications Thomson-Benard Phenomena In Relaxed Optics

Now we will discuss the problem of possible receiving and observation of Thomson-Benard phenomena in Relaxed Optics. First attempt of using the theory of Thomson-Benard phenomena for explanation the results of the generation the laser-induced hexagonal nanohills on diamond substrate of germanium was made my A. Medvid [30]. But receiving structures had volume nature in contrast to surface nature for the case classical Thomson-Benard phenomena [30]. We show that these experimental data may be explaining with help cascade model of excitation the proper chemical bonds in the regime of saturation the excitation [28].

We must see on the Thomson-Benard phenomena with physical-chemical point of view. In the case of liquid and electronic gas these phenomena has nonequilibrium nature in Relaxed Optics – irreversible nature. Therefore, we must represent the possible realization of these processes with help first kinetic concept of Relaxed Optics.

Firstly, we must estimate temporal and energetic characteristics of regimes the laser irradiation, which can be search of these processes according to first (kinetic) concept of Relaxed Optics [22].

The chain of hierarchy of corresponding times may be represented in next form. Let τ_i is the time of laser irradiation of matter; τ_h is the time of heat the irradiated matter to point of its melting; τ_m is the time of existing the melting phase, including heatind in liquid phase; τ_{TB} is the time of generation Thomson-Benard structures and its life, τ_c is cooling time of irradiated.

The time hierarchy for laser-induced Thomson-Benard phenomena is next

$$\tau_i << \tau_h < \tau_m << \tau_{TB} \sim \tau_c. \qquad (25)$$

Energy characteristic of irradiation is next: laser radiation must have self-absorption nature with absorption index ~ $10 \div 100$ cm^{-1} melting layer must be having sufficiently large value. This condition is necessary for the homogeneous power transmission of laser radiation to irradiated matter. So, irradiation of indium antimonide and indium arsenide by millisecond pulses of Ruby and Nedimium lasers (index absorption ~ 10^5 cm^{-1}) is connected with heterogeneous processes of phase transformations in irradiated matter, which is caused by the processes of second-order reradiation of first-order absorpting radiation [23]. For the observation of pure laser-induced Thomson-Benard phenomena, we must create the conditions of homogeneous absorption of light in subsurface region of irradiated matter. For the regimes of absorption the laser irradiation with absorption indexes ~ $10 \div 100\, cm^{-1}$, processes of second-order reirradiation have analogous absorption indexes. It is allow receiving homogeneous conditions of radiation in corresponding subsurface layer of irradiated matter. This regime of irradiation allows increasing the value of homogeneous depth (distribution) of irradiated matter.

Basic energies, which are characterized the laser-induced Thomson-Benard phenomena are next: E_{hs} – energy of heating the irradiated matter is solid phase to melting point; E_{hmh} – hidden melting heat; E_{TB} – energy of heating the laser-irradiated matter to point of generation the Thomson-Benard phenomena.

Thus, formula for full effective energy, which is necessary for the generation Thomson-Benard phenomena, may be represented as

$$E = E_{hs} + E_{hmh} + E_{TB}. \qquad (26)$$

This energy condition is very rough and has more “thermodynamic” as “laser” nature. But this estimation allows determining regimes of laser irradiation of corresponding matter, which are necessary for expected experimental data. In this case, we assumed that the laser-induced and thermodynamic processes of melting and the behavior of the molten material occur in the same way. This allows the use of thermodynamic methods to assess the energy exposure regimes. Naturally, in this approximation, the effective "thermodynamic" absorbed energy is proportional to the laser irradiation energy and can reach 40-50 percent of the incident radiation.

Roughly speaking conditions (25) and (26) allow receiving the “thermodynamic” nature of necessary regimes of laser irradiation.

The conditions of creation laser-induced frozen picture of Thomson-Benard phenomena are connected with next temporal correlation: lifetime of cells must more as time of cooling down of irradated matter.

In really, we can use specific heat of melting Q_{shm} and specific heat of vaporization Q_{shv}.. If we know the volume of melting material, then we can estimate the effective absorbing energy. For the observation the Thomson-Benard phenomena we can determine the rough threshold of its processes as Q_{TB} ~0,5Q_{shm}. Esxperimental values of corresponding regimes the irradiation may be receive after multiplication the corresponding heat on the volume of melting material V_m ant its densities. Corrresponding energiers we mark as E_{shm} and E_{TB}. We choose the size of the irradiated area as follows: diameter – 2 *cm*, and depth – 0,1 *cm*, volume – 0,314 cm^3.

Roughly speaking bond between corresponding specific heat and energy may be represented nwith help nexy formula

$$E_i = \frac{m}{m_{mol}} Q_i = \frac{V}{V_{mol}} Q_i, \qquad (27)$$

where m, m_{mol}, V, V_{mol} are mass and volume of transformed matter and one one mol, respectively.

The basic estimations these values of specific heats and corresponding enrergies for silicon, germanium, and titanium are represented in Table 1.

Table1. *Energies characteristics of laser-irradiated silicon, germanium, and titanium, which are necessary for its melting generation laser-induced Thomson-Benard phenomena and vaporization.*

	Q_{shm}, *kJ/mol*	Q_{shv}, *kJ/mol*	Q_{TB},	V_{mol}, cm^3/*mol*	E_{shm}, *kJ*	E_{TB}, *k J*	E_v, *kJ*
Silicon	50.6	383	192	12.1	1.312	4.982	9.964
Germanium	36.8	328	164	13.6	0.851	3.786	7.571
Titanium	18.8	422.6	211.3	10.6	0.557	6.259	12.518

The corresponding densities of enrgies, which are necessary for the breaking of proper numbers of coordination numbers (chemical bonds) in the regime of saturation thr excitatiion for silicon and germanium are represented in Table 2.

Table2. *Volume density of energy I_{vi} (10^3 J/cm^3), which is necessary for the breakage of proper number of chemical bonds in the regime of saturation of excitation in Si and Ge [3, 22, 28].*

	I_{v1}	I_{v2}	I_{v4}	I_{v5}
Si	12,8 – 14,4	25,6 – 28,8	51,2 – 57,6	63 – 72
Ge	6,3 – 8,4	12,6 – 16,8	25,2 – 33,6	31,5 – 42

If we multiplicate the data of Table 2 on volume 0.314 cm^3 than receive next results (Table 3).

Table3. *Energies E_i (kJ), which are necessary for the breakage of proper coordination numbers (chemical bonds) in the regime of saturation of excitation in Si and Ge for volume 0,314 cm^3 .*

	E_1	E_2	E_4	E_5
Si	4.019 – 4.525	8.038 – 9.050	16.076 – 18.100	20.095 – 27.150
Ge	1.978 – 2.637	3.955– 5.274	7.910 – 10.548	9.888 – 13.529

Experimental data by A. Medvid, which he wanted to explain as Benard phenomenon, are represented in Fig. 7 [30]. Samples of Ge {111} and Ge {001} i-type single crystals are used in experiment. Nd:YAG laser (wavelength 1,064 μm, duration of pulse 15 ns, pulse rate 12,5 Hz, power P=1 MW) was used for the irradiation. But the pictures of Fig. 2 and Fig. 7 are various. Therefore we must be search another ways of explanation the data of Fig. 7.

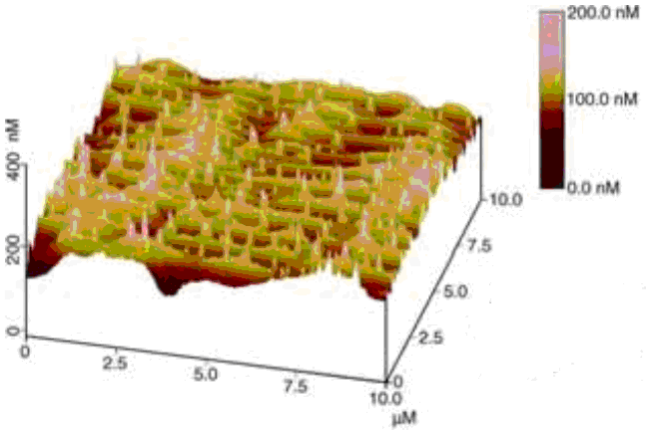

Fig7. *Three-dimensional AFM image of nanostructures after Nd:YAG laser irradiation with density of power 28 MW/cm^2 on Ge surface [30]*

Comparative analysis results of Table 1 and Table 3 show, that maximal values of energies, which are necessary for corresponding physical chemical transformations in laser-irradiated silicon and germanium, have similar values. Therefore, we must mark basic peculiarities of irradiation conditions for the receiving physical-chemical tranasformation irradiated matter to phase with more low crystal symmetry. Two multipulsr regimes of laser irradiation are effective: first nanosecond with absorption index $\sim 10^5 - 10^6 cm^{-1}$ Fig. 8a [31, 32]; and picosecond and femtosecond with absorption index $\sim 10^3 - 10^4 cm^{-1}$ (Fig. 8b) [33]. Roughly speaking, we must have only results for column E_2 of Table 3. But this results give integral value of energy, which is necessary for the breaking the two coordination numbers for the transition from diamond lattice to hexagonal. We must choose the experimental conditions so that the heating of the irradiated material must be insignificant. The first initial pulse must generate the emergence of a new phase, subsequent pulses lead to the growth of this phase, as well as the appearance of new phases on its surface (the hedgehog similar surface structures) [3, 28, 31-33]. New phases grow perpendicular to the surface of the previous phases. The surface has an irregular shape. Next conclusion was made: thermal processes in this case make an insignificant contribution to the final formation of structures. Really regimes of irradiation are ~ E_2 [3, 28, 31-33]. For more intensive regimes of irradiation E_4 and E_5 we can receive ablation or sublimation of irradiated materials [3, 28, 31-33]. Only multipulse regimes of irradiation allow receiving the cascade oh laser-induced physical-chemical phase transformations. These regimes must be without heating and melting or sublimation. It must they should be much faster than heating processes and even more melting of the irradiated material.

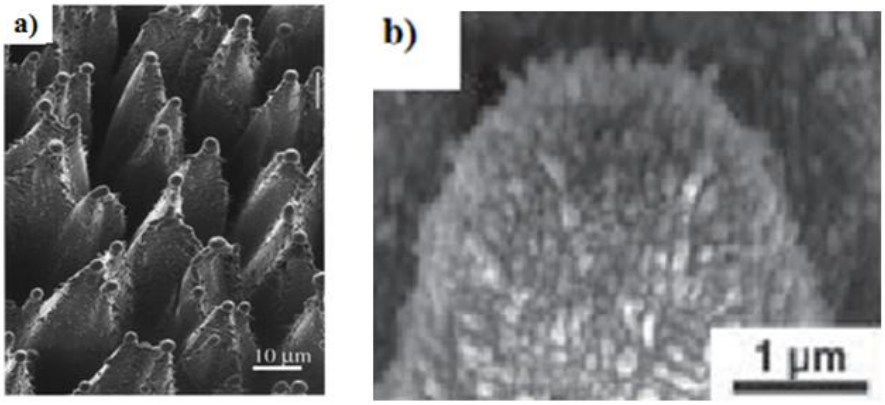

Fig8. *a) – Walled Si structures produced by 2040 laser pulses (E_d =1.5 J/cm^2, pulse duration 25 ns, vawelength 248 nm) in 1 atm of SF_6 [31, 32]; b) - Surface silicon nanocolumns of little scale, which have orthogonal orientation to a crests of nanorelief of large scale [33]*

For the Thomson-Benard phenomena we have another scenario. Main part of laser absorpted energy must be transformed in heating. Elements of crystalline or quasi-crystalline structures are presented in molten silicon and germanium [34]. Classical Thomson-Benard phenomena have more large scale as results of Fig. 8. Effects of Fig. 8 are undesirable for getting Thomson-Benard phenomena. We must receive conditions analogous to melting of spermaceti [5, 6] or paraftine [7]. After melting, the Thomson-Bénard structures are "frozen" with relatively rapid cooling.

Thus, the processes of creation laser-induced Thomson-Benard phenomena for multipulse regimes of irradiation are unlikely.

One of basic conditions of creation Thomson-Benard phenomena are homogeneous irradiation of fairly large areas of material. Depths more as one micron were investigated by Benard and his followers. Depths less as one micron were not investigated. Laser-induced generation of Thomson-Benard phenomena allow to determine spatial and temporal limits of these processes. Spatial limits must be determined by depth of melting layers; temporal – by irradiation time and time of generation the second-order processes.

Next direction of search Thomson-Benard phenomena is connected with including electromagnetic and shock processes in the formation of pre-vortexes and vortexes states. The influence of light polarization on laser-induced space distribution (interference pattern) is modeled with help V. Makin model of surface polariton-plasmons [35]. This model allows determining the period of interference pattern, but cannot explain its stratification. This question was resolved with help cascade model of excitation the proper chemical bonds (or centers of light scattering) in the regime of saturation the excitation [3, 22-28].

We can search other ways of realization the generation pre-vortexes structures with electromagnetic nature. First are hydromagnetic structures [1]. This method was used for the modeling of Sun spots and Sun activity [1]. Second is connected with concept of optical solitons [36]. But in Relaxed Optics we must connect these phenomena with phase transformations in laser-irradiated matter.

The Thomson-Benard phenomena with change gravitation interaction on electromagnetic with point of Thomson-Benard phenomena were stadied by V. Bonch-Bruevich and A. Temchin [18-20]. The formal analogy between nonlinear optical phenomena and second-order nonequilibrium phase transitions was noted by H. Haken [3, 12]. Therefore roughly speaking we can transit from nonequlibrium to irreversible processes and after this will be have processes of Relaxed Optics [3, 22-28].

As result we must search more complex universal methods for the more full and adequate representation and explanation of possible laser-induced pre-vortexes, including Thomson-Benard, processes and phenomena.

5. CONCLUSIONS

1. The short historical analysis of Thomson-Benard phenomena is represented.
2. Short review of main experimental data is made.
3. The role of gravitation field and thermal convection processes on the formation two dimensional polygonal pictures is investigated.
4. Rayleigh theory of these phenomena and its developments are analyzed.
5. The problem of Benard phenomena for hot electron gas in semiconductors are represented and observed.
6. Role of electromagnetic and thermal processes in the Relaxed Optical processes are estimated.
7. Conditions for the generation of Thomson-Benard processes in phenomena in the laser-irradiated matter are formulated.
8. Thus, we show, that laser-induced Thomson-Benard processes are dynamic process of Relaxed Optics.
9. Discussions of possible experiments are made.

10. Comparative analysis of conditions the irradiation for laser-induced physical-chemical processes and Thomson-Benard phenomena is represented.

REFERENCES

[1] Chandrasekar S. (1961) Hydrodynamic and Hydromagnetic Stability. Dover Publications, New York

[2] Karlov N., Kirichenko N. (2003) Oscillations, waves, structures. Phizmatlit, Moscow (in Russian)

[3] Trokhimchuck P. P. (2020) Relaxed Optics: Modeling and Discussions. Lambert Academic Publishing, Saarbrukken

[4] Thomson J. (1882). On a changing tesselated structure in certain liquids. Proceedings of the Philosophical Society of Glasgow. Vol. 8, Is. 2, 464–468.

[5] Bénard, Henri (1900). Les tourbillons cellulaires dans une nappe liquide Revue Générale des Sciences Pures et Appliquées. Vol. 11, 1261–1271, 1309–1328 (in French).

[6] Dynamic of Spatio-Temporal Cellular Structures. Henri Benard Centenary Review. Eds. Innocent Mutabazi Jose Eduardo Wesfreid Etienne Guyon. (2006). Springer Tracts of Modern Physics, vol. 207. Springer Science-Business Media, lnc., New York

[7] Rayleygh (J. W. Strutt) (1916) On convective currents in a horizontal layer of fluid then the higher temperature is on the under side. Philosoph. Mag., Vol. 32, 529-546.

[8] Rayleygh (J. W. Strutt) (1879) On the instability of Jets. London Math. Soc. Proc., Vol. X, 4-13.

[9] Pearson J.R.A. (1958). On convection cells induced by surface tension. Journal of Fluid MechanicsVol. 4, Is. 5, 489–500

[10] Ebeling W. (1979) Creation structures under irreversible processes. Mir publisher, Moscow (In Russian)

[11] Glensdorf P., Prigogine I. (2003) Thermodynamic theory of structure, stability and fluctuations. URSS, Moscow (In Russian)

[12] Haken H. (1980) Synergetics. Mir publisher, Moscow (In Russian)

[13] Getling A. V. (1991) Formation of spatial structures Rayleygh-Benard convections. Advance Physical Science. Vol. 161. №9, 1-80 (In Russian)

[14] Getling A. V. (1998). Bénard–Rayleigh Convection: Structures and Dynamics. World Scientific, Singapore

[15] Eckert, Kerstin; Bestehorn, Michael; Thess, André (1998). Square cells in surface-tension-driven Bénard convection: experiment and theory. Journal of Fluid Mechanics. Vol. 356, Is. 1, 155–197.

[16] Trenogin V. A., Yudovich V. I. (editors) (1974)., Theory of Bifurcation and Nonlinear Eigenvalue Problems, Mir, Moscow (in Russian)

[17] Gershuni G. Z., Zhukovitski E. M. (1972) Convective Instability of an Incompressible, Nauka, Moscow

[18] Bonch-Bruevich V. L. (1975) The Benard problems for hot electrons in semiconductors. Sov. Phys, JETP. Vol. 40, No. 6, 1092-1098.

[19] Temchin A. N. (1978) Benard phenomenon in semiconductors. Izvestiya Vysshykh Uchebnykh Zavedenii, Physica. No. 7, 41-45 (in Russian)

[20] Bonch-Bruevich V. L., Temchin A. N. (1979) Nonlinear theory of the electron temperature superlattice in semiconductors. Sov. Phys, JETP. Vol. 48, No. 5, 1713-1726.

[21] Bonch-Bruevich V. L, Zvyagin I. P., Mironov A. G. (1972) Domain Electric Instability in Semiconductors. Moscow, Nauka (in Russian)

[22] Trokhimchuck P. P. (2016) Relaxed Optics: Realities and Perspectives. Lambert Academic Publishing, Saarbrukken

[23] Trokhimchuck P. P. (2017) Problems of reradiation and reabsorption in Relaxed Optics. IJARPS. Vol. 4, Is. 2, 37 – 50

[24] Trokhimchuck P. P. (2018) Problems of modeling the phase transformations in Nonlinear and Relaxed Optics (review). IJERD. Vol.14, Is.2, 48-61

[25] Trokhimchuck P. P. (2018) Some Problems of Modeling the Volume Processes of Relaxed Optics. IJARPS. Vol. 5. Is. 11, 1-14

[26] Trokhimchuck P. P. (2020) Nonlinear Dynamical Systems. 2-d ed. Vezha-Print, Lutsk (In Ukrainian)

[27] Trokhimchuck P. P. (2018) Continuum mechanics. Vezha-Print, Lutsk (in Ukrainian)

[28] Trokhimchuck P. P. (2020) Role physical-chemical processes in the generation of laser-induced structures. Research trends in chemical sciences.Vol.11. Is. 6, AkiNik Publications, Delhy, 109-140

[29] Aleksenko A. G. (2014) Graphen. BINOM, Moscow (in Russian)

[30] Medvid' A. (2010) Nano-cones Formed on a Surface of Semiconductors by Laser Radiation: Technology, Model and Properties. In: Nanowires Science and Technology ed. Nicoletta Lupu. Inech, Vukovar, 61–82.

[31] Pedraza A. J., Fowlkes J. D., Lowndes D. H. (1999) Silicon microcolumn arrays growth by nanosecond pulse laser irradiation. Appl. Phys. Lett. 74(10), 2222-2224.

[32] Pedraza A. J., Guan Y. F., Fowlkes J. D., Smith D. A., Lowndes D. H. (2004) Nanostructures produced by ultraviolet laser irradiation of silicon. I. Rippled structures. J. Vac. Sc. @ Techn. B., vol. 22, no.10, 2823-2835.

[33] Shen M., Carey J. E., Crouch C. H., Kandyla M., Stone H. A., Mazur E. (2008) High-density regular arrays of nano-scale rods formed on silicon surfaces via femtosecond laser irradiation in water. Nanoletters, vol. 8, is. 7, 2087-2091.

[34] Magomedov Ya B., Gadzhiev G. G., Kollaev S. N. (2013) Thermophysical properties of silicon and its melt at high temperatures. Bulletin of the Dagestan Scientific Center. No. 49, 15-18.

[35] Makin V. S. (2013) Peculiarities of the formation the ordered micro and nanostructures in condensed matter after laser excitation of surface polaritons modes. D. Sc. Thesis. State university of information technologies, mechanics and optics, Saint-Petersburg (In Russian)

[36] Kivshar Yu., Agraval G. (2003) Optical solitons. Elsevier, New York a. o.

Citation: *Petro P. Trokhimchuck (2021). Thomson-Benard phenomena and Relaxed Optics. International Journal of Advanced Research in Physical Science (IJARPS) 8(3), pp.1-15, 2021.*